Polymer 51 (2010) 211–221

Contents lists available at ScienceDirect

Polymer

journal homepage: www.elsevier.com/locate/polymer

Lithium sulfonate promoted compatibilization in single ion conducting solid polymer electrolytes based on lithium salt of sulfonated polysulfone and polyether epoxy

Soma Guhathakurta, Kyonsuku Min*

Department of Polymer Engineering, The University of Akron, Akron, OH 44325-0301, USA

ARTICLE INFO

Article history:
Received 16 June 2009
Received in revised form
23 July 2009
Accepted 26 July 2009
Available online 6 August 2009

Keywords:
Lithium salt of sulfonated polysulfone
Single ion conducting
Polyether epoxy

ABSTRACT

Polymeric lithium salts of sulfonated polysulfone (SPSU(X)Li) were synthesized via post sulfonation route followed by ion exchange. A novel single ion conducting solid polymer electrolyte (SPE) was prepared by curing poly(ethylene glycol)diglycidyl ether (PEGDGE) with 4,4′ diaminodiphenyl sulfone (DDS) in SPSU(X)Li matrix. The ionic conductivity, thermal stability and tensile properties were investigated as a function of degree of sulfonation and PEGDGE concentration. The introduction of lithium sulfonate groups in polysulfone promoted compatibility of SPSU(X)Li and PEGDGE in SPE. AFM analysis demonstrated heterogeneous phase morphology and reduction in size of dispersed PEGDGE phase with increasing degree of sulfonation. The interactions between lithium sulfonate and polyether epoxy improved thermal stability of the epoxy network. The enhanced compatibility also caused improvement in elongation at break compared to neat SPSU(X)Li. The higher Li^+ ion concentration and the segmental mobility of the polymer chains above T_g contributed to the high ionic conductivity at high temperature in the single ion conducting SPE.

1. Introduction

Solid polymer electrolytes (SPE) have received great attention in the past two decades due to their potential applications in miniaturized electrochemical devices including rechargeable batteries, electrochromic windows and sensors. The use of polymer in developing electrolyte material combines ease of processability, design flexibility, light weight, shape versatility, safety and lack of toxicity [1–3]. Conventional solid polymer electrolytes are obtained by dissolving alkali metal salts in polyether matrix, first reported by Wright [4]. In such polymer electrolytes, the ether oxygen atoms interact with the cations (Lewis acid–base interactions) and cause salt solvation. The cation transport is assisted by segmental motion of the polymer chains. Recognizing the fact that ion conduction takes place in the amorphous phase of polyethylene oxide and ether oxygen atoms act as ion-coordinating sites [5,6], considerable research has focused on tailoring a flexible host polymer chemical structure with larger proportion of amorphous phase [7–11]. Liang et al. developed solid polymer electrolytes based on epoxide-crosslinked polysiloxane/polyether hybrid [9]. The conductivity and physical properties of the materials were modulated by coupling suitable amount of siloxane and ethylene oxide units along the host polymer backbone. The most promising SPE was developed by Armand and co workers using a weakly coordinating anion, bis(trifluoromethylsulfonyl)imide (TFSI) [1,12]. LiTFSI has the exceptional properties of an electrolyte salt; large electrochemical window, excellent oxidation resistance, high degree of dissociation due to low lattice energy of the salt and extensive negative charge delocalization.

The counter anions in the polymer electrolytes have weak interactions with the polyethers hence transport more easily compared to cations. Thus a major drawback of dual ion conducting SPEs is the low lithium ion transference number (0.3–0.5). The mobility of both cation and anion results polarization in practical application, which further reduces the Li^+ transference number. In addition, the mobile anions take part in undesirable side reactions at the electrodes. To date, two approaches have been reported to reduce the mobility of anions. The first one deals with introduction of interacting sites that preferentially interact with the anions [13,14] and in the other, anions are anchored to the polymer backbone [2,15,16]. The higher molecular weight of polyanions compared to Li^+ improves the cation transference number of the system. Development of amorphous single ion conducting solid polymer electrolyte with high molecular weight polyanion which can provide good thermal and mechanical stability was the main goal of present research.

The introduction of sulfonate groups in the polymer chain results specific interactions with complementary polar groups of other

* Corresponding author. Tel.: +1 330 972 6675; fax: +1 330 258 2339.
E-mail address: kmin@uakron.edu (K. Min).

0032-3861/$ – see front matter © 2009 Elsevier Ltd. All rights reserved.
doi:10.1016/j.polymer.2009.07.047

polymer and promote miscibility in polymer blends. Such interactions include hydrogen bonding, dipole–dipole, ion–dipole, charge transfer or transition metal complexation. Significant miscibility improvement was achieved in the blends of polyamide-6 and sulfonated polystyrene ionomers with lithium [17], zinc [18] and manganese [19] counter ions as a consequence of specific interactions between amide and sulfonate groups. Polysulfone (PSU) is a potential engineering thermoplastic due to its excellent thermal and chemical stability, mechanical strength, toughness and good film forming ability. Polysulfone (PSU)/polybenzimidazole (PBI) blends are immiscible while sulfonation of polysulfone at various degrees resulted miscible blends with PBI [20]. The miscibility was attributed to the specific interactions between N–H groups of PBI with sulfonate and sulfone groups of sulfonated polysulfone. Sodium sulfonated polysulfone formed miscible blends with polyamide 11 (polyundecanolactum) at a temperature close to the amide melting temperature [21]. Specific interactions between Na^+ and carbonyl oxygen atom and hydrogen bonding involving sulfonate and NH groups of amide were found to induce miscibility. Few studies have addressed the use of polyelectrolytes based on sulfonated polymers such as poly(lithium-4-styrene sulfonate) [22], poly(lithium 2 acrylamido-2-methyl propane sulfonate) [23] in single ion conducting SPE. However, conductivity is low in these materials and improves significantly in presence of a plasticizer [24].

Table 1
Sample designations and compositions of SPSU(*X*)Li/PEGDGE polymer electrolytes.

Sample designation	Degree of sulfonation (*X*)(%)	Wt (%) of SPSU(*X*)Li	Wt (%) of PEGDGE	[O]/[Li^+]
SPSU(23)Li/PEGDGE 100/0	23	100	0	0
SPSU(23)Li/PEGDGE 71/29	23	71	29	19
SPSU(23)Li/PEGDGE 56/44	23	56	44	36
SPSU(40)Li/PEGDGE 100/0	40	100	0	0
SPSU(40)Li/PEGDGE 71/29	40	71	29	11
SPSU(40)Li/PEGDGE 56/44	40	56	44	21
SPSU(76)Li/PEGDGE 100/0	76	100	0	0
SPSU(76)Li/PEGDGE 71/29	76	71	29	6
SPSU(76)Li/PEGDGE 56/44	76	56	44	12
SPSU(76)Li/PEGDGE 45/55	76	45	55	18
SPSU(76)Li/PEGDGE 33/67	76	33	67	30
SPSU(76)Li/PEGDGE 0/100	–	0	100	∞

In this paper, methodology to prepare a novel single ion conducting solid polymer electrolyte based on lithium salt of sulfonated polysulfone (SPSU(X)Li) and polyether epoxy, poly-

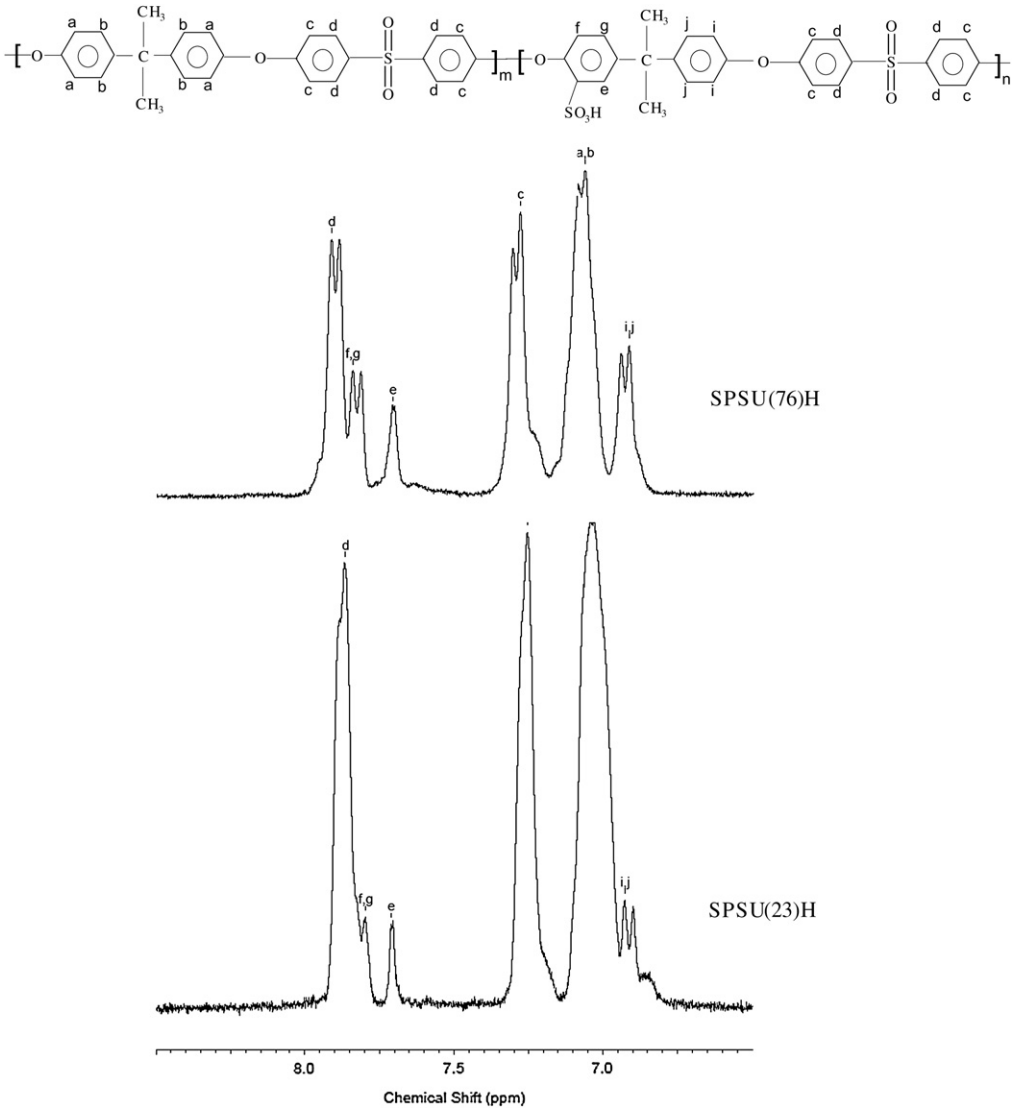

Fig. 1. . Proton NMR of sulfonated polysulfones at two different sulfonation levels (numbers within parenthesis refer to degree of sulfonation).

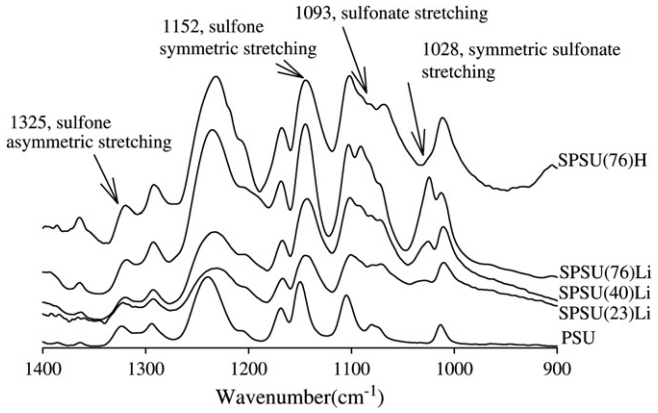

Fig. 2. . FT-IR spectra of lithium salt of sulfonated polysulfone at various sulfonation levels (numbers within parenthesis refer to degree of sulfonation).

(ethylene glycol)diglycidyl ether (PEGDGE) crosslinked by 4,4′ diaminodiphenyl sulfone (DDS) is described. The sulfonate ion induced compatibility of SPSU(X)Li and PEGDGE was studied as a function of sulfonation level and electrolyte composition. The morphology, thermal behavior, ionic conductivity and tensile properties were investigated and correlated with the compatibilization process in single ion conducting SPEs.

2. Experimental

2.1. Materials

Lithium salts of sulfonated polysulfone (SPSU(X)Li) were synthesized by post sulfonation of bisphenol A polysulfone followed by ion exchange in lithium hydroxide solution. Polysulfone (UDEL^{RM} P-1700) was provided by Solvay Advanced Polymers, L.L.C. The polymer was dried at 130 °C for 8–9 h in a vacuum oven. The sulfonating agent, trimethylsilylchlorosulfonate (TMSCS), lithium ion solvent, poly(ethylene glycol) diglycidyl ether (PEGDGE) and the curing agent, 4,4′ diaminodiphenyl sulfone (DDS) were purchased from Aldrich Chemical Co. The sulfonation was carried out in methylene chloride (Fisher Chemical), dried over molecular sieves prior to the reaction. Dimethylacetamide (DMAc) (Aldrich Chemical Co) was used for film casting.

2.2. Procedure

2.2.1. Sulfonation of bisphenol A polysulfone

The synthesis procedure of sulfonation is the same as described in the previous publication for sulfonated bisphenol A polyetherimide [25]. The homogeneous solution after the reaction was precipitated in methanol/isopropanol depending on the sulfonation level instead of acetone used for polyetherimide. The precipitate was filtered, washed with the respective non solvent and dried under vacuum at 90 °C for 24 h. The degree of sulfonation, *X* was controlled by varying the mole ratio of the sulfonating agent to the PSU repeat unit and/or the reaction time.

2.2.2. Preparation of lithium ion conducting solid polymer electrolytes

Sulfonated polysulfone in acid form, SPSU(X)H was dissolved in dimethylacetamide (DMAc) and the films were casted in glass Petridish. The solvent was evaporated at 60–70 °C in hood and then dried under high vacuum initially at ~60 °C for 4–5 h followed by 120 °C for 24 h. Lithium salt of sulfonated polysulfone SPSU(X)Li was prepared by soaking a dry film of SPSU(X)H in 0.1 N lithium hydroxide solution at ambient temperature for 24 h.

SPSU(X)Li and polyether epoxy, PEGDGE were dissolved in DMAc and the stoichiometric amount of curing agent, DDS was added to the mixture. The polymer electrolyte compositions are described in Table 1. The solutions were stirred for 2 h and the films were casted on Teflon coated aluminium boats followed by drying at 70 °C in the hood. The films were further dried at 60 °C for 48 h under vacuum (−28 in Hg) to remove the trace amount of solvent. The film thickness was controlled by using the same solution concentration and boats of same size. The samples were cured at 120–150 °C for 6–7 h in the oven. The lithium salt of sulfonated polysulfones with three different sulfonation levels 23, 40 and 76% were used in solution blending with polyether epoxy. The lithium ion concentration in the SPEs was expressed as the molar ratio of ether oxygen of PEGDGE to lithium sulfonate of SPSU(X)Li, [O]/[Li$^+$].

2.3. Characterization

The sulfonation reaction was quantified by ^{1}H Nuclear magnetic resonance (^{1}H NMR) using ~3% (w/v) DMSO-d_6 solution at room temperature. All spectra were recorded by Varian 300 MHz. The lithium sulfonated polysulfones and the intermolecular interactions in SPSU(X)Li/PEGDGE were characterized by Fourier

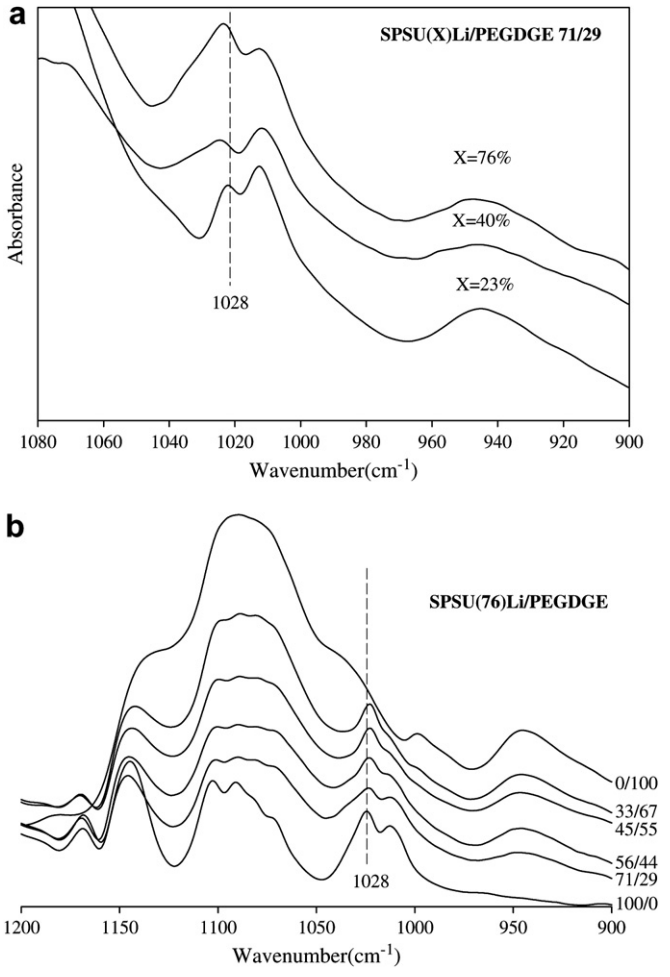

Fig. 3. a. FTIR spectra of SPSU(X)Li/PEGDGE 71/29, showing effect of degree of sulfonation (*X*) on symmetric stretching band of sulfonate group. b. FTIR spectra of SPSU(X)Li/PEGDGE polymer electrolytes in 900–1200 cm^{-1} stretching region at different PEGDGE weight percent.

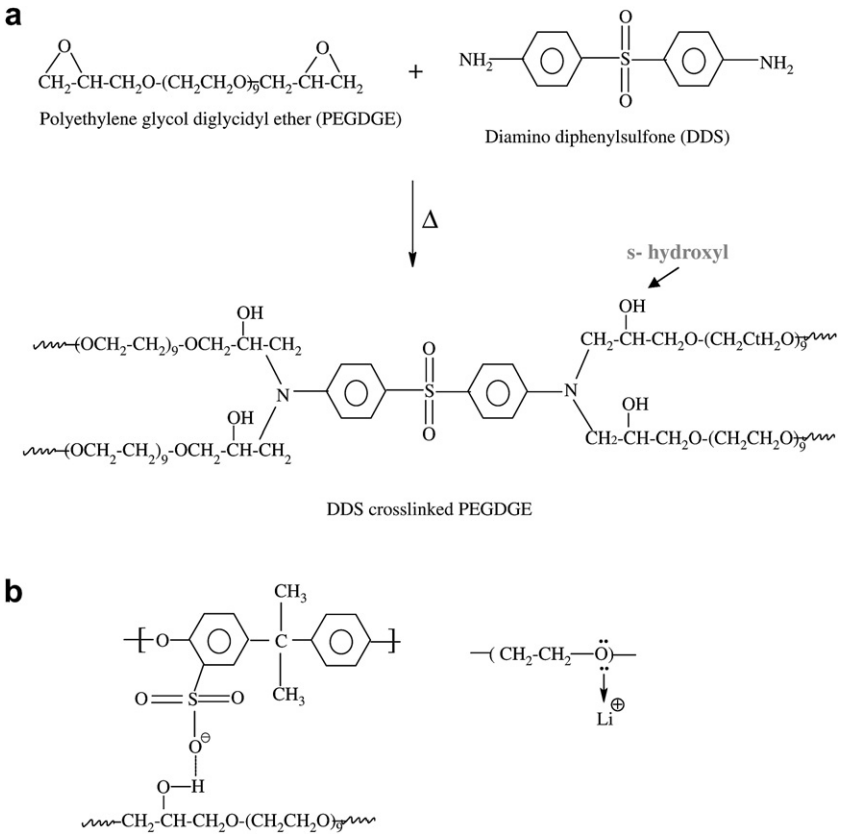

Fig. 4. a. Schematic structure of polyethylene glycol diglycidyl ether (PEGDGE) network crosslinked by diaminodiphenyl sulfone (DDS). b. Intermolecular interactions in SPSU(*X*)Li/PEGDGE polymer electrolytes.

transform infrared (FTIR) spectroscopy in attenuated total reflection (ATR) mode utilizing Nicolet 380 FTIR. The experiments were carried out in the absorbance mode in the wavelength range of 400–4000 cm^{-1} with 32 scans and a resolution of 4 cm^{-1}.

The morphology of SPE films was studied by atomic force microscopy (AFM) in tapping mode using Multi Mode Scanning Probe Microscope model with a Nanoscope IIIa Controller. The samples of SPSU(X)Li/PEGDGE for AFM were prepared by solution blending of the desired amount of SPSU(X)Li, PEGDGE and DDS in DMAc. The films were casted on AFM puck. The solvent was evaporated at 70 °C in hood and then at ~60 °C in a vacuum oven for 48 h. The films were cured at 120–150 °C for 6–7 h in the oven. AFM was operated using silicon cantilever probes with spring constant of 20–80 N m^{-1} and the resonance frequency in the range of 250–300 kHz. The topography and phase images were recorded simultaneously at room temperature with constant integral and proportional gain.

Differential scanning calorimetry (DSC) measurements were conducted by TA 2920 DSC. The glass transition temperatures of SPSU(X)Li and SPEs were determined at a heating rate of 10 °C/min under nitrogen atmosphere. In the first scan, the dry films were heated from room temperature to 150 °C and held isothermally at 150 °C for 30 min to remove the volatiles. The samples were heated to 300 °C in the second scan. All experiments were carried out with 10–12 mg sample, sealed in aluminium hermetic pans. The thermograms of second scan are provided.

Thermal degradation temperatures of the parent polymers and SPEs were determined utilizing Thermal Advantage Q500 modulated thermogravimetric analyzer (TGA) at a heating rate of 10 °C/min. The samples were heated from room temperature to 800 °C under nitrogen atmosphere.

Tensile tests were conducted using an Instron 5567 tensile testing machine with a crosshead speed of 50 mm/min. The tensile properties were determined following ASTM D 882 – 02 with a slight modification: the gage length was maintained at 25 mm in all cases and a paper holder was used to prevent grip slippage. The gauge length and the width of the specimens were 25 and 5 mm respectively. After mounting the specimen film supported by the paper holder onto the tensile testing machine, the two straps of the holder were cut prior to the testing so that the tensile load applied to the film.

2.4. Measurement of ionic conductivity

The ionic conductivity was determined using Hewlett Packard 4274A impedance analyzer operated in the frequency range 100 Hz–100 kHz. In the two terminal method, a polymer electrolyte film was sandwiched between two stainless steel blocking electrodes, and the magnitude of impedance, $|Z|$ and the phase angle, θ were obtained. The bulk resistance of the film was taken as the value of Z' (real axis) corresponding to the minimum imaginary response (Z''). The temperature dependent ionic conductivity was studied by attaching the electrode–electrolyte assembly to a hot stage using a heating rate of 10 °C/min in the temperature range of 30–160 °C.

3. Results and discussion

3.1. Characterization of sulfonated polysulfones by ^{1}H NMR and FTIR spectroscopy

^{1}H NMR spectra of sulfonated polysulfone (SPSU) at two different sulfonation levels are shown in Fig. 1. The singlet at 7.71 ppm (e)

corresponding to the protons adjacent to the sulfonic acid group and two doublets at 6.94 (i, j) and 7.84 ppm (f, g) associated with the sulfonated bisphenol A unit indicate successful introduction of sulfonic acid group in the activated bisphenol A moiety. The degree of sulfonation (DS) was determined by ^{1}H NMR in DMSO-d_6 [26]. The analysis based on the chemical structure of SPSU is that there are 16 aromatic protons in the non-sulfonated repeat unit and 14 aromatic protons in the sulfonated repeat unit with one proton adjacent to sulfonic acid group at 7.71 ppm. Since the peak at 7.71 ppm is well resolved from all other peaks, R is defined as the ratio of the area under the peak at 7.71 ppm, A_e, to the sum of the area under the peaks corresponding to all other aromatic protons, A. The degree of sulfonation is determined by the following equation:

$$\mathrm{DS} = \frac{16R}{1+2R}, R = \frac{A_e}{A} \quad (1)$$

Fig. 2 depicts FTIR spectra of lithium salts of sulfonated polysulfone at different degrees of sulfonation, 23, 40 and 76%. The prominent absorption peaks at 1028 and 1093 cm^{-1} associated with symmetric stretching of sulfonate group can be seen, the intensity of the bands increases with increasing sulfonation level. FTIR spectrum of sulfonated polysulfone in acid form, SPSU(76)H is also provided in Fig. 2. Comparing SPSU(76)Li with SPSU(76)H extensive hydrogen bond formation in SPSU(76)H causes broad absorption band at 1028 cm^{-1} masked by the diphenyl ether stretching vibration at 1014 cm^{-1}, while in SPSU(76)Li, prominent well resolved absorption peak at 1028 cm^{-1} is visible.

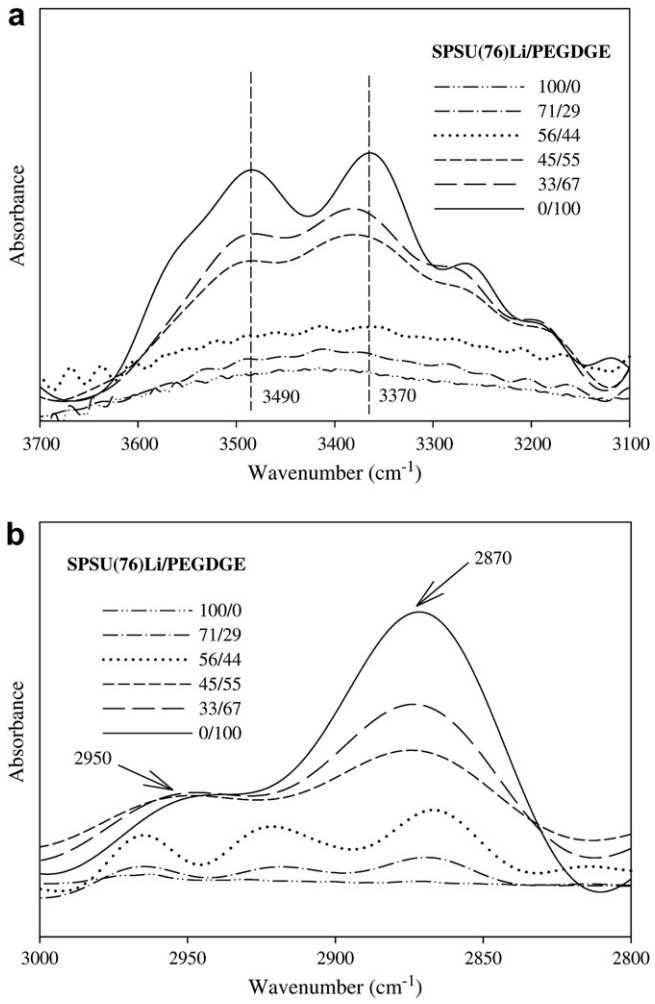

Fig. 5. a. FTIR spectra of O–H stretching region for SPSU(X)Li/PEGDGE polymer electrolyte at different epoxy weight percent. b. FTIR spectra showing C–H stretching region for SPSU(X)Li/PEGDGE polymer electrolyte at various epoxy weight percent.

3.2. Analysis of intermolecular interactions in single ion conducting polymer electrolytes

In present study, the symmetric sulfonate stretching band at 1028 cm^{-1} of SPSU has been used to monitor the specific intermolecular interactions in SPSU(X)Li/PEGDGE single ion conducting polymer electrolytes. The effect of sulfonation level on the peak maxima is described in Fig. 3a. The peak shows a slight blue shift and the width of the band increases with increasing degree of sulfonation reflecting a broad distribution of vibration frequencies of sulfonate groups in the presence of polyether epoxy. Fig. 3b shows FTIR spectra of SPSU(76)Li/PEGDGE in 900–1200 cm^{-1} region as a function of PEGDGE concentration. In all compositions, disappearance of epoxide characteristic band at 912 cm^{-1} indicates complete curing of epoxy network. The following spectral changes are observed: (a) the peak at 1014 cm^{-1} attributed to the symmetric stretching of diphenyl ether units, exhibits a decrease in intensity with decreasing SPSU(76)Li concentration, (b) the sulfonate symmetric stretching band located at 1028 cm^{-1} in all compositions shows a slight red shift. The crosslinking of PEGDGE by DDS is depicted in Fig. 4a. The secondary hydroxyl groups generated through crosslinking formed hydrogen bonds with sulfonate groups in SPSU matrix, shown in Fig. 4b. The sulfonate ions associated with hydroxyl groups through hydrogen bonding appear at higher frequency than the non-associated ones and the hydroxyl associated and non-associated sulfonate bands overlapped causing peak broadening. The observed blue shift of sulfonate stretching band with increasing degree of sulfonation was due to the strengthening of S=O bond of sulfonate group due to its interaction with hydroxyl groups of PEGDGE.

The high frequency deconvoluted spectra of SPSU(76)Li/PEGDGE as a function of epoxy concentration is displayed in Fig. 5a and b. The bands located at 3490 and 3370 cm^{-1} are attributed to free and hydrogen bonded hydroxyl groups respectively in crosslinked epoxy network (Fig. 5a). The intensity of hydroxyl stretching bands increases with increasing PEGDGE concentration indicating formation of larger number of secondary hydroxyl groups through DDS crosslinking. It is also seen in Fig. 5a that the peak corresponding to free hydroxyl stretching remains unchanged in SPSU(76)Li/PEGDGE while the hydrogen bonded hydroxyl stretching shifts slightly to higher wave number in 45/55 and 33/67 compositions with peak broadening. The increase in width of the band suggests that a certain fraction of hydroxyl groups were involved in hydrogen bonding with sulfonate anions and the blue shift of hydroxyl bands implies stronger sulfonate–hydroxyl ion–dipole interaction than the hydroxyl–hydroxyl and/or hydroxyl–ether dipole–dipole interactions in crosslinked PEGDGE network.

Several studies have reported the influence of cation complexation on COC and CH_2 absorption bands in polyethylene oxide–salt complexes [27–29]. In this study, analysis of COC asymmetric stretching region (1050–1125 cm^{-1}) (Fig. 3b) of the polyether epoxy was difficult due to the presence of characteristics bands of SPSU(76)Li in the same region. The effect of PEGDGE concentration on C–H stretching in SPSU(76)Li/PEGDGE is described in Fig. 5b. The peak at 2870 and 2950 cm^{-1} show an increase in intensity with gradual blue shift of the peak at 2870 cm^{-1} upon increasing PEGDGE content. A new peak is clearly seen at ~2925 cm^{-1} in 56/44 while at higher epoxy concentration (>44 wt%) it overlaps with the band at 2950 cm^{-1}. The ether oxygen atoms (Lewis base) of PEGDGE were co-ordinated to Li^+ ions of lithium sulfonate groups. The Lewis acid–base interaction caused strengthening of C–H bond in SPSU(76)Li/

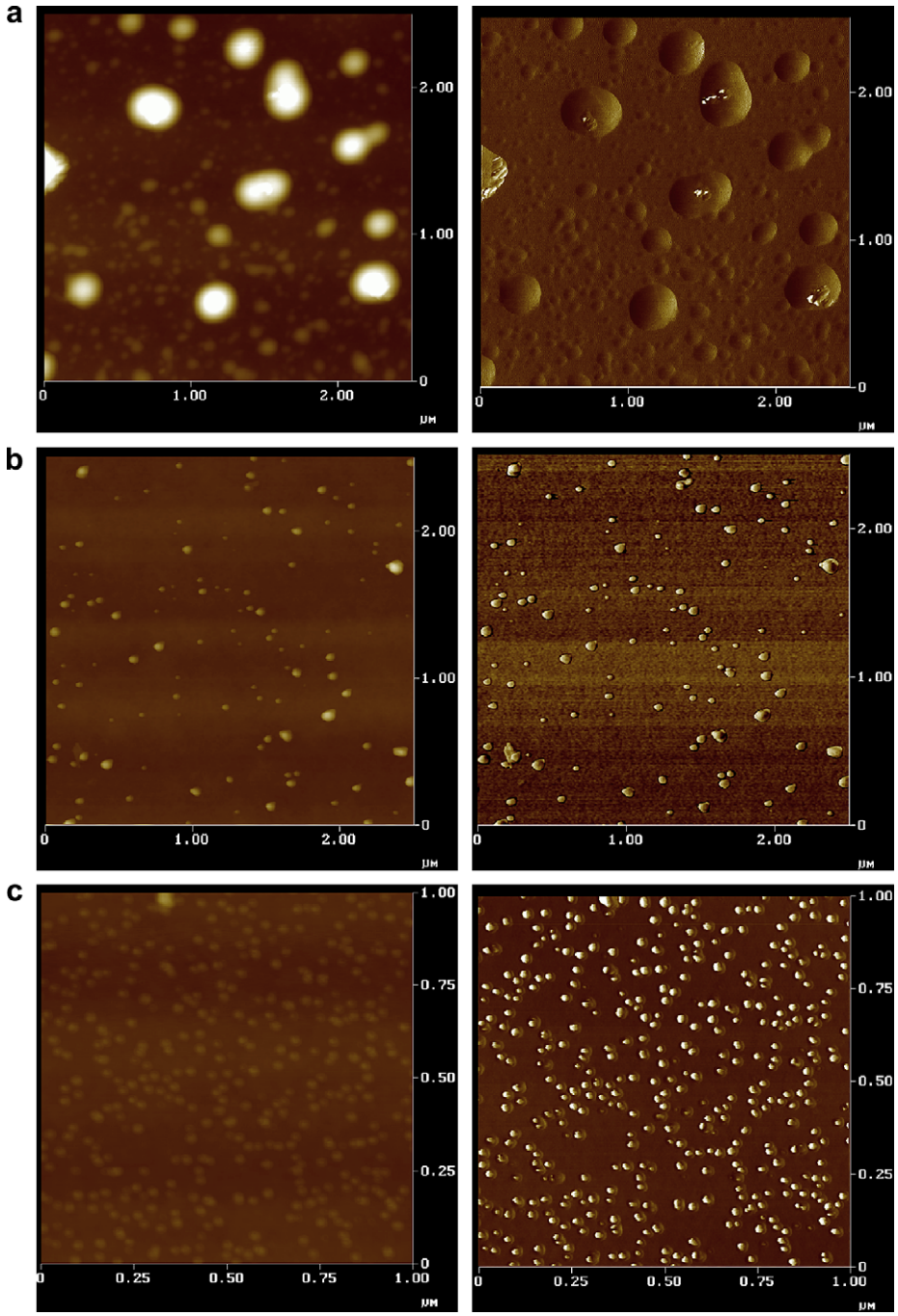

Fig. 6. Tapping mode height (left) and phase images (right) of SPSU(*X*)Li/PEGDGE 71/29 at various degrees of sulfonation (a) $X = 23\%$, (b) $X = 40\%$, (c) $X = 76\%$.

PEGDGE than in bulk PEGDGE network and the concentration of complexed polyether chains increased with increasing PEGDGE content.

3.3. Morphology

Fig. 6 shows AFM images (topographic (left) and phase image (right)) of 71/29 composition at various sulfonation levels. The heterogeneous phase morphology is observed in all samples. It should be pointed out that the scan size for the samples with 76% sulfonation level is smaller (1.00 μm) than those with 23 and 40% (2.5 μm). The size of the dispersed epoxy phase significantly reduces and the size distribution becomes narrower with increasing degree of sulfonation. The effect of PEGDGE content on phase morphology of SPSU(76)Li/PEGDGE are shown in Figs. 6c and 7. The images demonstrate increase in size of the dispersed phase and in 33/67 composition more "co-continuous" phase morphology is evident as the larger amount of epoxy phase masks the SPSU domains, shown in Fig. 7b. It is also apparent that the variation in height is responsible for the observed phase contrast. 71/29 compositions have domains with relatively circular cross section of average diameter ranging from 40 to 350 nm.

As mentioned earlier, the polar hydroxyl and ether groups of crosslinked epoxy phase interact with sulfonate and Li^+ ions of SPSU(*X*)Li. The extent of interactions increased with increasing sulfonate ion concentration and caused reduction in size of the

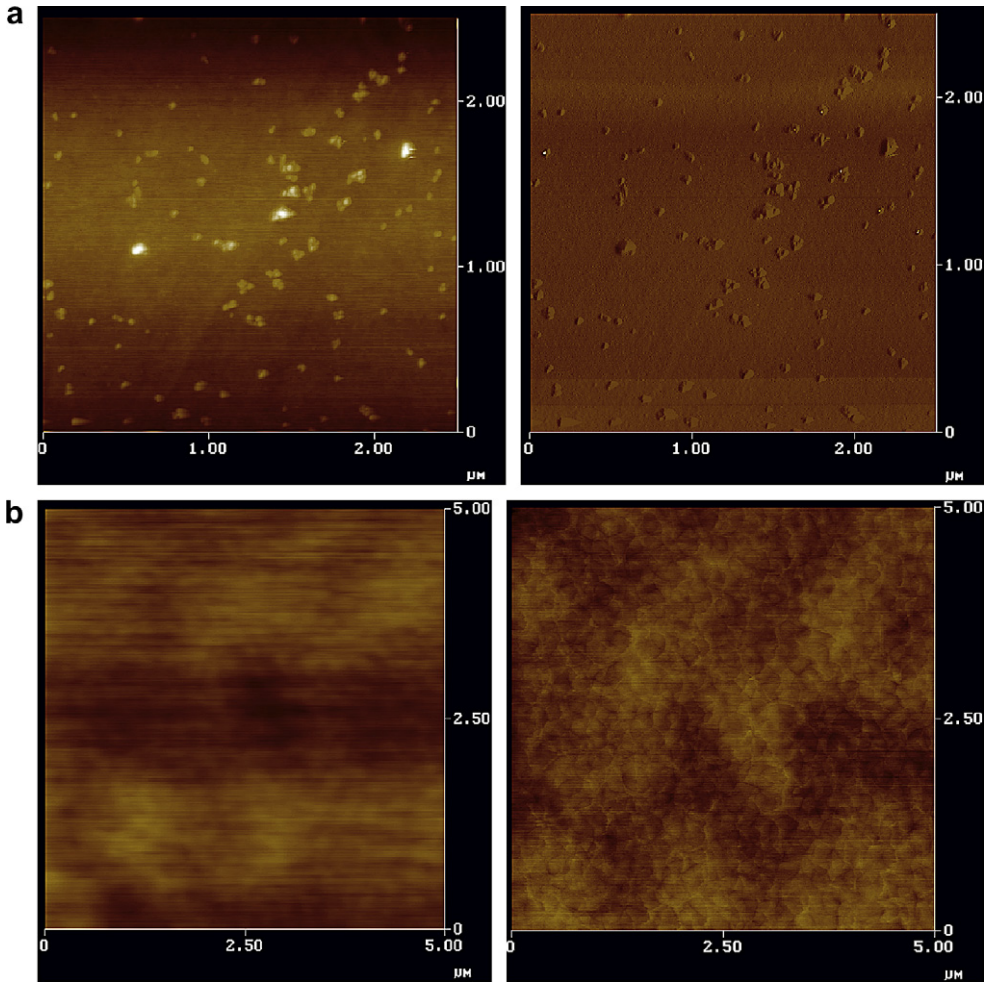

Fig. 7. Tapping mode height (left) and phase images (right) of SPSU(76)Li/PEGDGE for two different polymer electrolyte compositions (a) 56/44, (b) 33/67.

dispersed epoxy phase. The wide distribution of domain size in SPSU(23)Li/PEGDGE 71/29 and increase in size with PEGDGE concentration in SPSU(76)Li/PEGDGE also indicate that a certain fraction of polyether epoxy was involved in specific interactions with SO_3Li depending on the degree of sulfonation and/or PEGDGE weight percent. The free polyether chains that did not participate in any interaction due to insufficient sulfonate groups formed larger domains in sulfonated polysulfone matrix.

The optical clarity also provides an indication of miscibility in polymer blends [30,31]. Fig. 8 shows clarity of three representative sample specimens. All SPSU(*X*)Li/PEGDGE films were transparent except the samples with 23% sulfonation level. This can be attributed to the domain size of epoxy phase in SPSU(*X*)Li matrix smaller than the visible light at higher sulfonation level (40 and 76%). The larger size domains caused loss of optical clarity in SPSU(23)Li based samples.

3.4. Thermal analysis

Thermogravimetric analysis (TGA) was used to study the thermal stabilities of SPSU(*X*)Li/PEGDGE polymer electrolytes. The temperature corresponding to the peak on derivative-weight (%) vs. temperature curve, T_d, is provided in Table 2. DDS curing improves the degradation temperature of PEGDGE due to incorporation of diphenyl sulfone crosslinks in the epoxy network. The lithium salts of sulfonated polysulfone, SPSU(*X*)Li also exhibited higher thermal stability than the corresponding acid forms. The example cited for SPSU(76)Li and SPSU(76)H in Fig. 9, significant degradation takes place above 460 °C compared to 320 °C in the respective acids. The presence of PEGDGE in SPSU(*X*)Li matrix shows a two step degradation, T_{dI}, associated with the decomposition of crosslinked epoxy network and T_{dII} corresponds to the decomposition of SPSU(*X*)Li phase as shown in Fig. 10a. The degradation temperature of epoxy

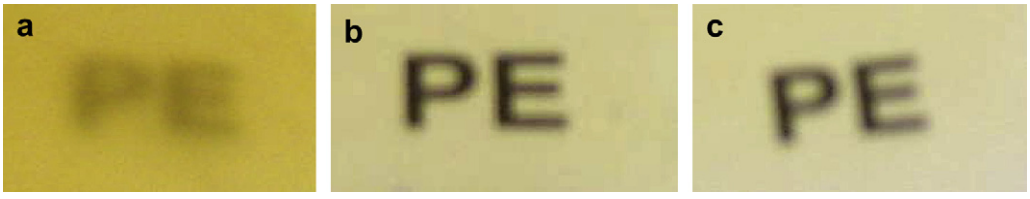

Fig. 8. Optical clarity of SPSU(X)Li/PEGDGE 71/29 at various sulfonation levels (a) $X = 23\%$, (b) $X = 40\%$, (c) $X = 76\%$. In each case the film was kept on a white paper with PE written on it.

Table 2
Thermal degradation of SPSU(*X*)Li/PEGDGE polymer electrolytes.

Sample designation	Thermal degradation(°C)	
	T_{dI}	T_{dII}
SPSU(23)Li/PEGDGE 100/0		499.7
SPSU(23)Li/PEGDGE 71/29	320.5	468.2
SPSU(23)Li/PEGDGE 56/44	322.1	467.4
SPSU(40)Li/PEGDGE 100/0	–	469.8
SPSU(40)Li/PEGDGE 71/29	352.8	472.2
SPSU(40)Li/PEGDGE 56/44	339.9	468.2
SPSU(76)Li/PEGDGE 100/0	–	502.9
SPSU(76)Li/PEGDGE 71/29	356.8	464.97
SPSU(76)Li/PEGDGE 56/44	367.3	458.5
SPSU(76)Li/PEGDGE 45/55	369.7	454.5
SPSU(76)Li/PEGDGE 33/67	377	449.6
PEGDGE (uncrosslinked)	368.1	–
PEGDGE (DDS crosslinked)	399.6	–

phase improves with increasing degree of sulfonation. The effect of epoxy concentration on thermal degradation is described in Fig. 10b. T_{dI} shows an increasing trend with increasing PEGDGE weight percent while T_{dII} decreases with increasing epoxy concentration. This behavior can be explained in terms of stronger ion–dipole interactions between PEGDGE and SO_3Li groups as evident in FTIR spectra compared to the dipole–dipole interactions in the pure epoxy network. The physical crosslinks resulted improved the thermal stability of epoxy phase.

Fig. 11a shows the DSC thermograms of SPSU(*X*)Li at various sulfonation levels. T_g of lithium salt of sulfonated polysulfone gradually increases and broadens with increasing degree of sulfonation. The specific interactions between lithium sulfonate groups caused immobilization of polymer chains resulting in an increase in T_g. SO_3Li groups were randomly located along the polymer chains and each individual chain did not have the same number of sulfonate groups. Thus, sulfonated polysulfone chains at higher sulfonation level underwent relaxation at higher temperature than those at lower degree of sulfonation. The wide distribution of relaxation temperatures was responsible for the broadening of glass transition.

The thermal transitions in SPSU(*X*)Li/PEGDGE are depicted in Fig. 11b. A transition is evident in the temperature range 0–100 °C in all samples; the inflection point shifts to a lower temperature with increasing PEGDGE concentration. The transition is broad in SPSU(*X*)Li/PEGDGE compared to the bulk epoxy network. The width of glass transition, ΔT_g is defined as the difference between

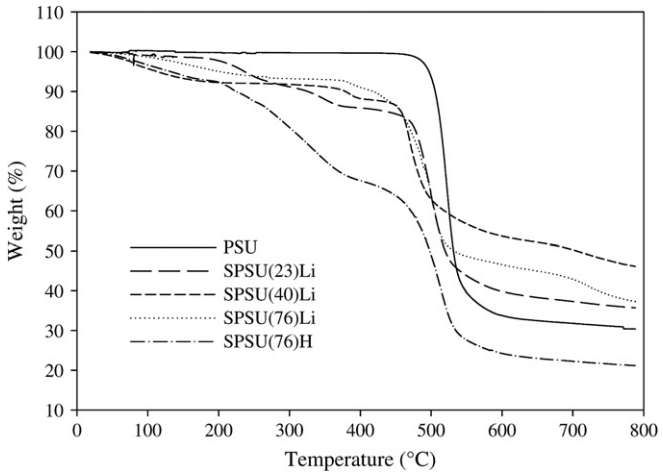

Fig. 9. TGA thermograms of sulfonated polysulfones at various sulfonation levels.

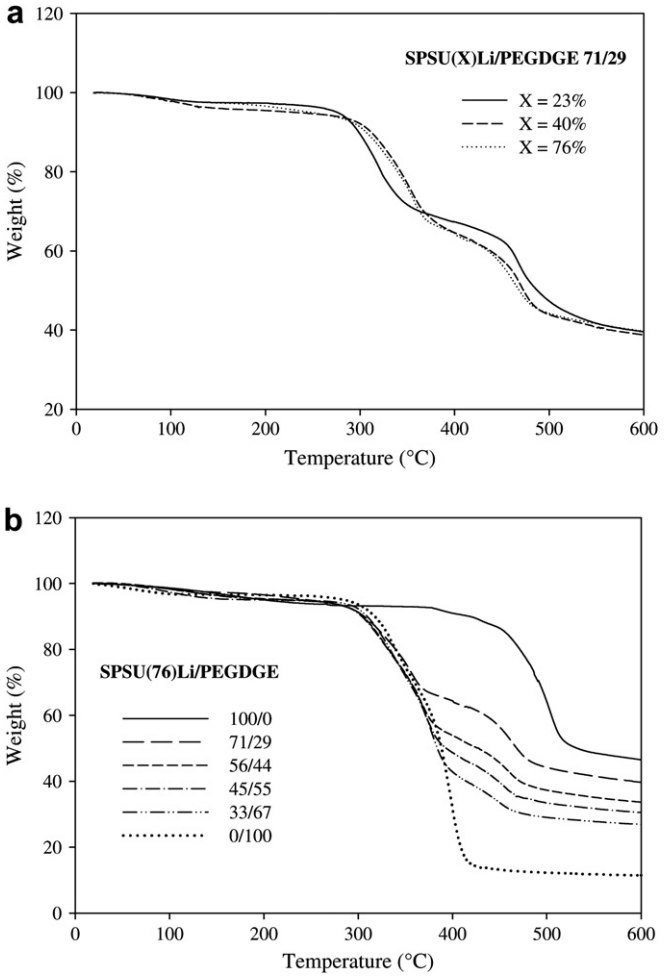

Fig. 10. a. TGA thermograms of SPSU(*X*)Li/PEGDGE 71/29 at various sulfonation levels. b. TGA thermograms of SPSU(76)Li/PEGDGE at different PEGDGE concentrations.

the onset and end point of transition and corresponds to the relaxation temperature distribution of the polymer chains. ΔT_g decreases upon increasing PEGDGE content. Thus the observed transition is assigned to the T_g of PEGDGE network. The complexed polyether chains in SPSU(*X*)Li matrix formed through ion–dipole interactions between SO_3Li and hydroxyl/ether oxygen of PEGDGE underwent relaxation at a higher temperature than free polyether segments and the wide distribution of relaxation temperatures resulted broad thermal transition. With increasing PEGDGE concentration, the larger number of free polyether chains caused T_g of the epoxy phase shift towards that of bulk network and simultaneously reduced ΔT_g.

Two thermal transitions are evident in SPSU(*X*)Li/PEGDGE 71/29. The inflection point in the same temperature range as in SPSU(23)Li (T_g ~202.6 °C) was due to sulfonated polysulfone chains that did not participate in any interaction with PEGDGE due to insufficient ion exchange sites (lithium sulfonate). The larger domains of the dispersed epoxy phase observed in AFM images (Fig. 6a) were formed by the free polyether chains in SPSU(23)Li matrix. ΔT_g can be correlated to distribution of the domain size as the broad transition is observed for SPSU(23)Li/PEGDGE 71/29, the sample with wide domain size distribution. The thermal transition associated with the T_g of SPSU(76)Li phase was not detected in SPSU(76)Li/PEGDGE due to the broad transition in neat lithium sulfonated polysulfones at higher sulfonation levels (Fig. 11a) and dilution effect.

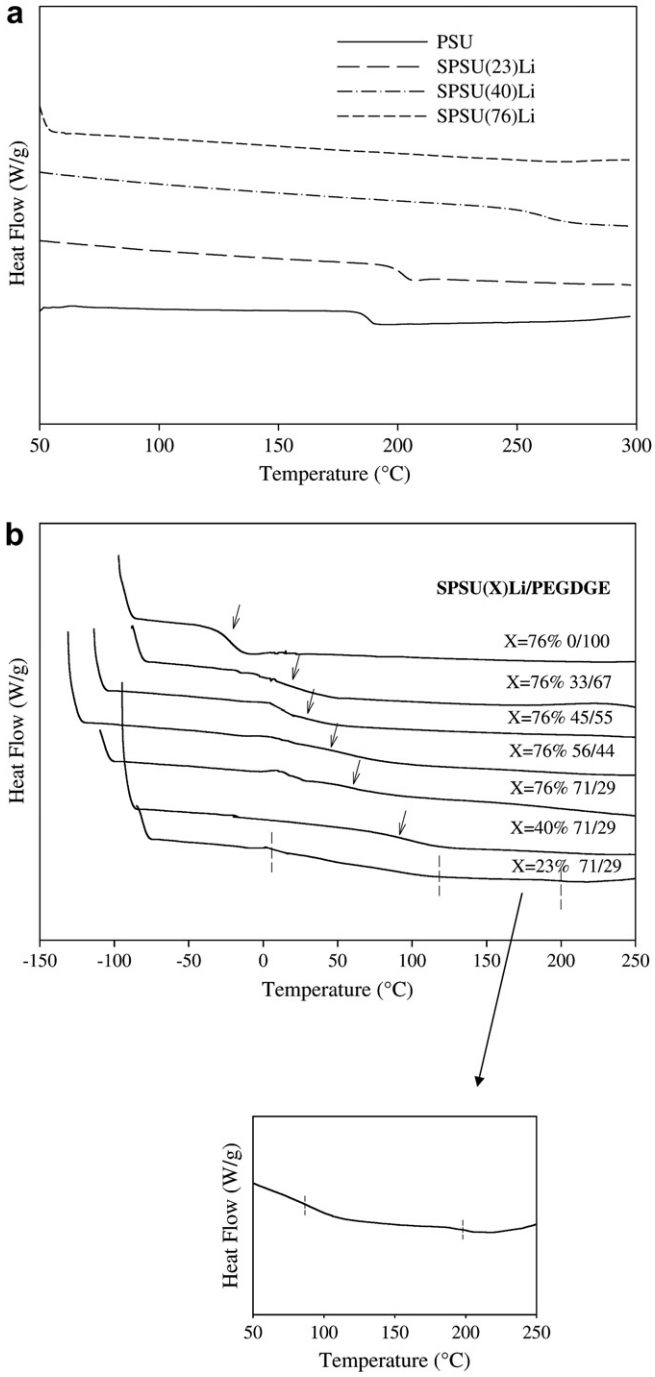

Fig. 11. a. DSC thermograms of lithium sulfonated polysulfones at different sulfonation levels. b. DSC traces of SPSU(*X*)Li/PEGDGE polymer electrolytes.

3.5. Ionic conductivity

The temperature dependence of ionic conductivity (σ) of polymer electrolytes was studied as a function of degree of sulfonation and PEGDGE content (Fig. 12). At a given PEGDGE concentration (44 wt%), conductivity increases drastically with increasing sulfonation level. Fig. 12 also exhibits the influence of PEGDGE content on the ionic conductivity of SPSU(76)Li/PEGDGE. At a lower temperature ($\sim$30 °C), there is little variation in conductivity except in 33/67 composition. At a high temperature the difference is prominent and σ increases with SPSU(76)Li weight percent. Fig. 13a and b illustrates random distribution of lithium sulfonate (SO_3Li) in SPSU(*X*)Li matrix

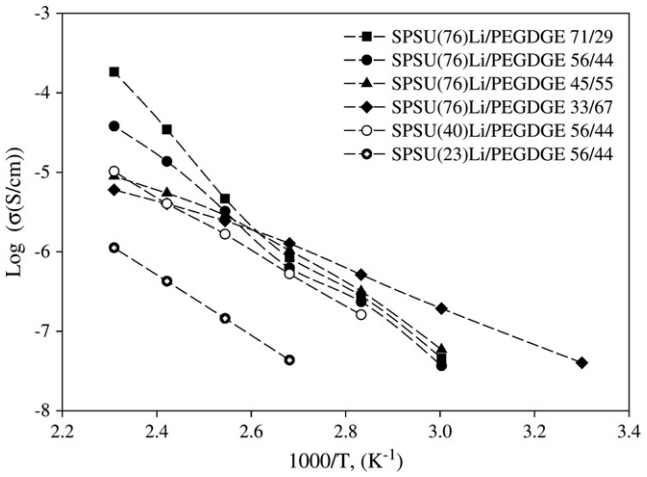

Fig. 12. Temperature dependent ionic conductivity of SPSU(*X*)Li/PEGDGE at various degrees of sulfonation, *X* and polymer electrolyte compositions.

and phase separation in SPSU(*X*)Li/PEGDGE polymer electrolyte at intermediate PEGDGE concentration respectively. Li^+ ion conduction mechanism within each domain is shown by an arrow. The transport of Li^+ ions in SPSU(*X*)Li/PEGDGE occurred in PEGDGE phase and SPSU(*X*)Li acted as Li^+ ion donor. The concentration of charge carriers and segmental mobility of polyether chains are the two determinants of ionic conductivity. SO_3Li groups were mainly located at the interface due to the ion–dipole interactions with polyether epoxy which also caused dissociation of the polymeric lithium salt. These solvated free Li^+ ions were the major contributors to conductivity. At a lower temperature ($\sim$30 °C), the conductivity was high in 33/67 compositions since its glass transition temperature was below room temperature. The influence of lesser number of charge carriers due to lower salt content was compensated by the larger free volume available for the segmental motion. At a higher temperature (>120 °C), conductivity increases with increasing Li^+ ion concentration as the difference between segmental mobility was less pronounced beyond the glass transition temperature of the matrix. At 160 °C, σ reaches the value of 10^{-4} S/cm for 71/29 composition. It is also apparent in Fig. 12 that the Arrhenius plots of the temperature dependence of conductivity deviate from linearity at high temperature indicative of ionic conductivity coupled with segmental motion of polyether chains of PEGDGE above T_g. The less deviation from linearity for 33/67 composition implies segmental mobility varied slightly with temperature in the sample.

3.6. Tensile properties

The stress–strain plots of SPSU(X)Li/PEGDGE are shown in Fig. 14. Neat SPSU(*X*)Li samples used in this study exhibit a gradual reduction in strength and modulus with increasing sulfonation level. We intended to measure the tensile properties of DDS cured PEGDGE but these materials failed at the grip due to their poor tensile strength. It is apparent from Fig. 14 that the presence of crosslinked epoxy phase in SPSU(*X*)Li shows a significant improvement in elongation at break while reduces the tensile strength and modulus. The increased PEGDGE concentration in SPSU(76)Li/PEGDGE caused the system to transform from brittle to ductile behavior. The results can be correlated with the increase in size of PEGDGE phase at 76% degree of sulfonation as described in Figs. 6 and 7, beyond 55 wt% epoxy content, the tensile properties approached those of bulk epoxy network and the elongation at break declines.

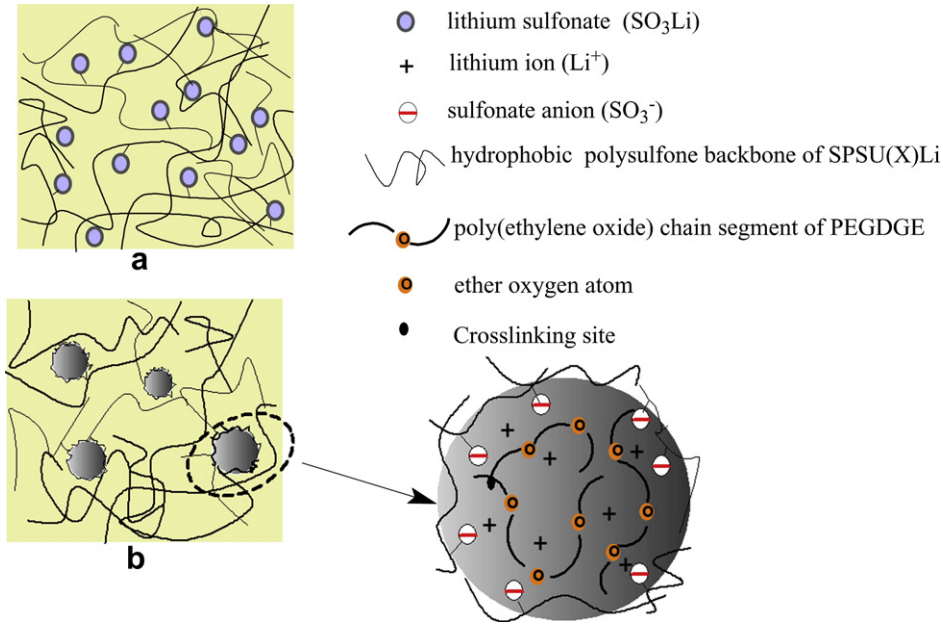

Fig. 13. Schematic illustration of lithium ion conduction mechanism in single ion conducting polymer electrolytes. (a) random distribution of lithium sulfonate in SPSU(*X*)Li matrix, (b) phase separation in SPSU(*X*)Li/PEGDGE at intermediate PEGDGE concentration. Lithium ion conduction mechanism within the dispersed epoxy phase is shown by an arrow.

The effect of sulfonation level on tensile properties for 71/29 composition indicates that SPSU(*X*)Li/PEGDGE at higher sulfonation level has larger elongation at break than those with low sulfonate content. With increasing degree of sulfonation, the specific interactions between SPSU(*X*)Li and polyether epoxy were predominant. Lithium sulfonate promoted compatibility of the two components in SPSU(*X*)Li/PEGDGE resulted reduction in dispersed phase size and better interfacial adhesion, thus improvement in elongation at break. The presence of 55 wt% epoxy was better than 67% in improving the elongation at break. It may be due to the fact that 55 wt% epoxy saturated almost all the sulfonate ion exchange sites located at the interface between SPSU(76)Li and PEGDGE phases, beyond this concentration the tensile properties deteriorated. A similar behavior was reported in previous studies. Su et al. described the role of hydroxyl functional groups in promoting in situ compatibilization between functionalized polystyrene (PS) and polybutylene terephthalate (PBT) [32,33]. Weber et al. reported in situ formation of polysulfone (PSU)–polyamide (PA) copolymer upon addition of phthalic anhydride terminated PSU, was responsible for particle size reduction of PA dispersed phase and caused significant toughness improvement in reactive PA/PSU blends [34].

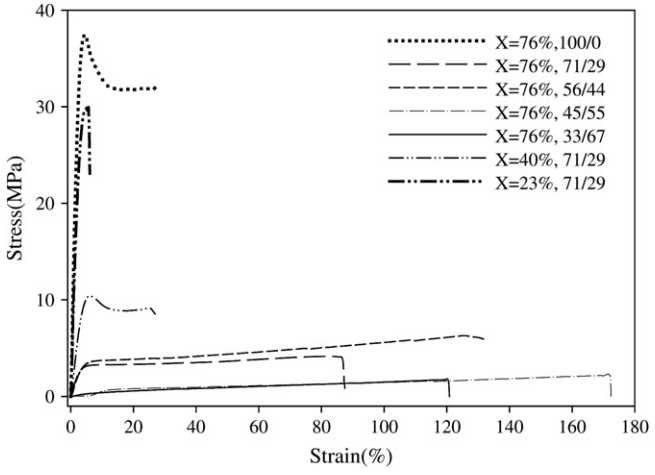

Fig. 14. Stress–strain plots of SPSU(*X*)Li/PEGDGE polymer electrolytes.

4. Conclusions

Lithium salts of sulfonated polysulfone at three different sulfonation levels were synthesized via post sulfonation route using trimethylsilylchlorosulfonate followed by ion exchange in lithium hydroxide solution. The sulfonation reaction at the activated bisphenol A moiety was evident from ^{1}H NMR spectra. Solvent free single ion conducting solid polymer electrolytes were prepared by crosslinking a polyether epoxy, poly(ethylene glycol)diglycidyl ether (PEGDGE) by 4,4′ diaminodiphenyl sulfone (DDS) in SPSU(*X*)Li matrix. FTIR spectroscopy demonstrated specific interactions between SO_3Li of SPSU(*X*)Li, ether and hydroxyl groups of PEGDGE which caused significant shift in T_g of epoxy network. The interactions were also found to be responsible for the improved thermal stability of PEGDGE in the sulfonated polymer matrix compared to the bulk. Higher concentration of sulfonate ions improved the compatibility of SPSU(*X*)Li and PEGDGE. The enhanced compatibility caused size reduction of the dispersed epoxy phase. The presence of crosslinked PEGDGE in SPSU(*X*)Li matrix improved the elongation at break but had detrimental effect on tensile strength and modulus. The Arrhenius plots for the temperature dependent ionic conductivity of the polymer electrolytes showed deviation from linearity at high temperature implying ionic conductivity assisted by the segmental mobility of the polymer chains occurred above the glass transition temperature. The ionic conductivity reached $\sim 10^{-4}$ S/cm in SPSU(76)Li/PEGDGE 71/29 at 160 °C suitable for application in electrochemical devices operating at high temperature.

Acknowledgement

The authors would like to acknowledge State of Ohio Third Frontier Program (ODOD # 07-029) for the financial support to conduct this research work.

References

[1] Tarascon J-M, Armand M. Nature 2001;414:359.
[2] Gray FM. Polymer electrolytes. Cambridge: The Royal Society of Chemistry; 1997.
[3] MacCallum JR, Vincent CA, editors. Polymer electrolyte reviews 1 and 2. London: Elsevier; 1987 and 1989.
[4] Fenton DE, Parker JM, Wright PV. Polymer 1973;14:589.
[5] Armand A. Solid State Ionics 1994;69:309.
[6] Koksbang R, Olsen II , Shackle D. Solid State Ionics 1994;69:320.
[7] Meyer WH. Adv Mater 1998;10:439.
[8] Andreev YG, Bruce PG. Electrochim Acta 2000;45:1417.
[9] Liang WJ, Kuo P-L. Macromolecules 2004;37:840.
[10] Watanabe M, Rikukawa M, Sanui K, Ogata N. Macromolecules 1986;19:188.
[11] Kuo P-L, Liang W-J, Chen T-Y. Polymer 2003;44:2957.
[12] Armand M, Gorecki W, Anreani R. In: Scrosati B, editor. Second international symposium on polymer electrolytes. London and New York: Elsevier; 1990.
[13] Lee HS, Yang XQ, Xiang CL, McBreen J. J Electrochem Soc 1998;145:2813.
[14] Zhang SS, Angel CA. J Electrochem Soc 1996;143:4047.
[15] Ganapathiappan S, Chen K, Shiver DF. Macromolecules 1988;21:2299.
[16] Fujinami T, Tokimoto A, Mehta MA. Chem Mater 1997;9:2236.
[17] Molnar A, Eisenberg A. Polymer Commun 1991;32:370.
[18] Lu X, Weiss RA. Mater Res Soc Symo Proc 1991;215:29.
[19] Lu X, Weiss RA. Macromolecules 1991;24:4381.
[20] Deimede V, Voyiatzis GA, Kallitsis JK, Qingfeng L, Bjerrum NJ. Macromolecules 2000;33:7609.
[21] Deimede VA, Fragou KV, Koulouri EG, Kallitsis JK, Voyiatzis GA. Polymer 2000;41:9095.
[22] Park CH, Sun Y-K, Kim D-W. Electrochim Acta 2004;50:375.
[23] Sun J, MacFarlane DR, Forsyth M. Solid Sate Ionics 2002;147:333.
[24] Hardy LC, Shriver DF. Macromolecules 1984;17:975.
[25] Guhathakurta S, Min K. Polymer 2009;50:1034.
[26] Bai Z, Houtz MD, Mirau PA, Dang TD. Polymer 2007;48:6598.
[27] Chintapalli S, Quinton C, Frech R, Vincent CA. Macromolecules 1997;30:7472.
[28] Wen SJ, Richardson TJ, Ghantous DI, Striebel KA, Ross PN, Cairns EJ. J Electroanal Chem 1996;408:113.
[29] Marzantowicz M, Dygas JR, Krok F, Nowiński F, Tomaszewska A, Florjańczyk Z, et al. J Power Sources 2006;159:420.
[30] Goh SH. Polym Bull 1987;17:221.
[31] Avakian RW, Allen RB. Polym Eng Sci 1985;25:62.
[32] Su W-Y, Wang Y, Min K, Quirk RP. Polymer 2001;42:5107.
[33] Su W-Y, Min K, Quirk RP. Polymer 2001;42:5121.
[34] Charoensirisomboon P, Weber M. Polymer 2001;42:7009.